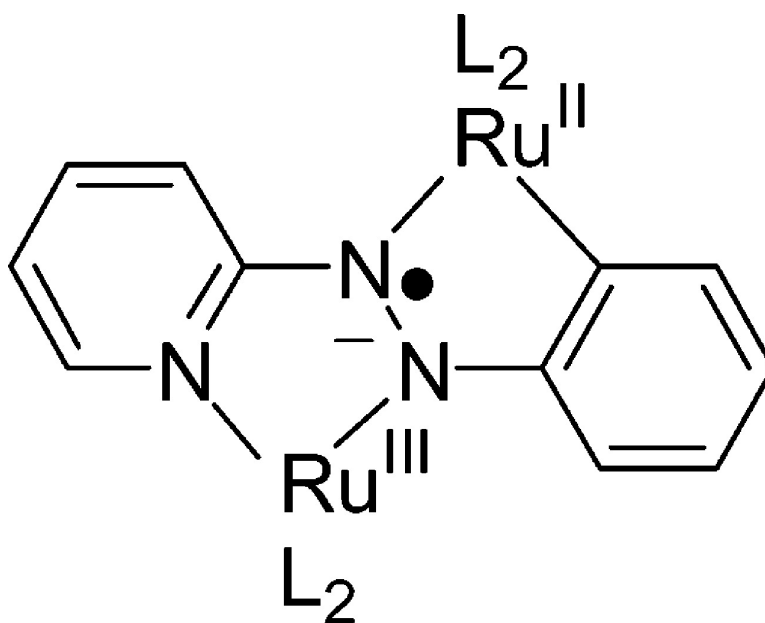Article

Mixed-Valent Metals Bridged by a Radical Ligand: Fact or Fiction Based on Structure-Oxidation State Correlations

Biprajit Sarkar, Srikanta Patra, Jan Fiedler, Raghavan B. Sunoj,
Deepa Janardanan, Goutam Kumar Lahiri, and Wolfgang Kaim

More About This Article

Additional resources and features associated with this article are available within the HTML version:

- Supporting Information
- Links to the 3 articles that cite this article, as of the time of this article download
- Access to high resolution figures
- Links to articles and content related to this article
- Copyright permission to reproduce figures and/or text from this article

View the Full Text HTML

Mixed-Valent Metals Bridged by a Radical Ligand: Fact or Fiction Based on Structure-Oxidation State Correlations

Biprajit Sarkar,[†] Srikanta Patra,[‡] Jan Fiedler,[§] Raghavan B. Sunoj,*,[‡]
Deepa Janardanan,[‡] Goutam Kumar Lahiri,*,[‡] and Wolfgang Kaim*,[†]

*Institut für Anorganische Chemie, Universität Stuttgart, Pfaffenwaldring 55, D-70550 Stuttgart,
Germany, Department of Chemistry, Indian Institute of Technology, Bombay, Powai,
Mumbai-400076, India, and J. Heyrovský Institute of Physical Chemistry, v.v.i., Academy of
Sciences of the Czech Republic, Dolejškova 3, CZ-18223 Prague, Czech Republic*

Received October 5, 2007; E-mail: sunoj@chem.iitb.ac.in; lahiri@chem.iitb.ac.in; kaim@iac.uni-stuttgart.de
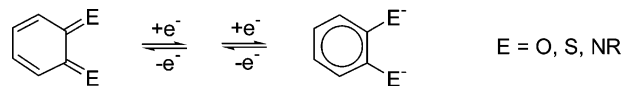
Abstract: Electron-rich $Ru(acac)_2$ ($acac^- = 2,4$-pentanedionato) binds to the π electron-deficient bis-chelate ligands L, L = 2,2′-azobispyridine (abpy) or azobis(5-chloropyrimidine) (abcp), with considerable transfer of negative charge. The compounds studied, $(abpy)Ru(acac)_2$ (**1**), *meso*-(μ-abpy)$[Ru(acac)_2]_2$ (**2**), *rac*-(μ-abpy)$[Ru(acac)_2]_2$ (**3**), and (μ-abcp)$[Ru(acac)_2]_2$ (**4**), were calculated by DFT to assess the degree of this metal-to-ligand electron shift. The calculated and experimental structures of **2** and **3** both yield about 1.35 Å for the length of the central N–N bond which suggests a monoanion character of the bridging ligand. The NBO analysis confirms this interpretation, and TD-DFT calculations reproduce the observed intense long-wavelength absorptions. While mononuclear **1** is calculated with a lower net ruthenium-to-abpy charge shift as illustrated by the computed 1.30 Å for d(N–N), compound **4** with the stronger π accepting abcp bridge is calculated with a slightly lengthened N–N distance relative to that of **2**. The formulation of the dinuclear systems with monoanionic bridging ligands implies an obviously valence-averaged $Ru^{III}Ru^{II}$ mixed-valent state for the neutral molecules. Mixed valency in conjunction with an anion radical bridging ligand had been discussed before in the discussion of MLCT excited states of symmetrically dinuclear coordination compounds. Whereas **1** still exhibits a conventional electrochemical and spectroelectrochemical behavior with metal centered oxidation and two ligand-based one-electron reduction waves, the two one-electron oxidation and two one-electron reduction processes for each of the dinuclear compounds $Ru^{2.5}(L^{\bullet-})Ru^{2.5}$ reveal more unusual features via EPR and UV–vis–NIR spectroelectrochemistry. In spite of intense near-infrared absorptions, the EPR results show that the first reduction leads to $Ru^{II}(L^{\bullet-})Ru^{II}$ species, with an increased metal contribution for system $4^{\bullet-}$. The second reduction to $Ru^{II}(L^{2-})Ru^{II}$ causes the disappearance of the NIR band. One-electron oxidation of the $Ru^{2.5}(L^{\bullet-})Ru^{2.5}$ species produces a metal-centered spin for which the alternatives $Ru^{III}(L^0)Ru^{II}$ or $Ru^{III}(L^{\bullet-})Ru^{III}$ can be formulated. The absence of NIR bands as common for mixed-valent species with intervalence charge transfer (IVCT) absorption favors the second alternative. The second one-electron oxidation is likely to produce a dication with $Ru^{III}(L^0)Ru^{III}$ formulation. The usefulness and limitations of the increasingly popular structure/oxidation state correlations for complexes with noninnocent ligands is being discussed.
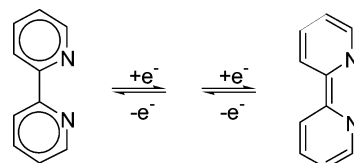
Introduction

The use of structural parameters to establish oxidation states of ligands and, by implication, of coordinating metals has become a popular exercise for transition metal compounds with potentially noninnocent ligands.[1] The chelating *o*-quinone/*o*-semiquinone/catecholate type redox system of Scheme 1 has been most thoroughly studied,[2,3] and statistically derived guidelines to aid in structure-oxidation state correlations were presented.[2b,c]

In the absence of aromatic stabilization which can favor the reduced form (as in Scheme 1) or the oxidized state (as in

---

[†] Universität Stuttgart.
[‡] Indian Institute of Technology.
[§] J. Heyrovský Institute of Physical Chemistry, v.v.i.
(1) (a) Ward, M. D.; McCleverty, J. A. *J. Chem. Soc., Dalton Trans.* **2002**, 275. (b) Chaudhuri, P.; Verani, C. N.; Bill, E.; Bothe, E.; Weyhermüller, T.; Wieghardt, K. *J. Am. Chem. Soc.* **2001**, *123*, 2213.

Scheme 1

E = O, S, NR

Scheme 2

Scheme 2, 2,2′-bipyridine (bpy) behaving as a noninnocent ligand), the chelating 1,4-diazabutadiene/1,2-enediamido redox systems (Scheme 3) were shown by computationally supported structure analysis to function as noninnocent ligands not only toward main group elements but also toward transition metals.[4]
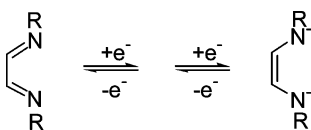
Scheme 3

Scheme 4

Scheme 5

$$E=E \; \underset{-e^-}{\overset{+e^-}{\rightleftharpoons}} \; \underset{-e^-}{\overset{+e^-}{\rightleftharpoons}} \; {}^-E-E^-$$
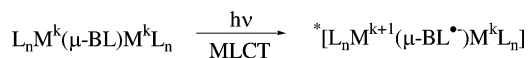
$$E = O, NR$$
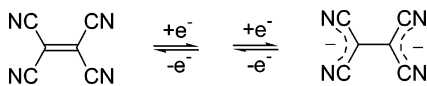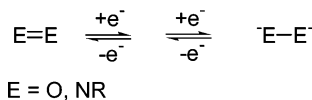
A corresponding approach was described recently[5a] in detail for the potentially fourfold metal-bridging[6] $TCNE^{0/\bullet-/2-}$ redox system (TCNE = tetracyanoethene, Scheme 4) which can produce a variety of magnetic and nonmagnetic coordination compounds.[5,6]

One of the simplest noninnocent ligand systems involves the double bond/single bond conversion in Scheme 5 where E = O represents the biologically important dioxygen species $O_2{}^{n-}$.[7]

Azo compounds (diazenes) also fall into the category of Scheme 5 with E = NR; enhanced stability and additional potential for coordination are obtained when R is a 2-pyridyl,[8] related heteroaryl,[9] acyl,[10] or imine[11] substituent.

In the course of studying the coordination chemistry of 2,2′-azobispyridine (abpy)[8] we have recently obtained and structurally characterized the two diastereoisomers, *meso* and *rac* forms, of $(acac)_2Ru(\mu\text{-abpy})Ru(acac)_2$ (acac⁻ = acetylacetonato = 2,4-pentanedionato).[12] The N−N bond lengths of about 1.36 Å were

(2) (a) Pierpont, C. G.; Lange, C. W. *Prog. Inorg. Chem.* **1994**, *41*, 331. (b) Pierpont, C. G. *Coord. Chem. Rev.* **2001**, *219−221*, 415. (c) Bhattacharya, S.; Gupta, P.; Basuli, F.; Pierpont, C. G. *Inorg. Chem.* **2002**, *41*, 5810. (d) Lever, A. B. P.; Gorelsky, S. L. *Struct. Bonding* **2004**, *107*, 77. (e) Mitra, K. N.; Choudhury, S.; Castiñeiras, A.; Goswami, S. *J. Chem. Soc., Dalton Trans.* **1998**, 2901.

(3) (a) Haga, M.; Dodsworth, E. S.; Lever, A. B. P. *Inorg. Chem.* **1986**, *25*, 447. (b) Masui, H.; Lever, A. B. P.; Auburn, P. *Inorg. Chem.* **1991**, *30*, 2402. (c) Ebadi, M.; Lever, A. B. P. *Inorg. Chem.* **1999**, *38*, 467. (d) Lever, A. B. P.; Auburn, P. R.; Dodsworth, E. S.; Haga,. M.; Liu, W.; Melnik, M.; Nevin, W. A. *J. Am. Chem. Soc.* **1988**, *110*, 8076. (e) Auburn, P. R.; Dodsworth, E. S.; Haga, M.; Liu, W.; Nevin, W. A.; Lever, A. B. P. *Inorg. Chem.* **1991**, *30*, 3502. (f) Bag, N.; Pramanik, A.; Lahiri, G. K.; Chakravorty, A. *Inorg. Chem.* **1992**, *31*, 40. (g) Bag, N.; Lahiri, G. K.; Basu, P.; Chakravorty, A. *J. Chem. Soc., Dalton Trans.* **1992**, 113. (h) Kokatam, S.; Weyhermüller, T.; Bothe, E.; Chaudhuri, P.; Wieghardt, K. *Inorg. Chem.* **2005**, *44*, 3709.

(4) (a) Greulich, S.; Kaim, W.; Stange, A.; Stoll, H.; Fiedler, J.; Zalis, S. *Inorg. Chem.* **1996**, *35*, 3998 and literature cited. (b) Muresan, N.; Weyhermüller, T.; Wieghardt, K. *Dalton Trans.* **2007**, 4390 and literature cited.

(5) (a) Miller, J. S. *Angew. Chem.* **2006**, *118*, 2570; *Angew. Chem., Int. Ed.* **2006**, *45*, 2508. (b) Bagnato, J. D.; Shum, W. W.; Strohmeier, M.; Grant, D. M.; Arif, A. M.; Miller, J. S. *Angew. Chem.* **2006**, *118*, 5448; *Angew. Chem., Int. Ed.* **2006**, *45*, 5322. (c) Manriquez, J. M.; Yee, G. T.; McLean, R. S.; Epstein, A. J.; Miller, J. S. *Science* **1991**, *252*, 1415.

(6) Kaim, W.; Moscherosch, M. *Coord. Chem. Rev.* **1994**, *129*, 157.

(7) Cotton, F. A.; Wilkinson, G.; Murillo, C. A.; Bochmann, M. *Advanced Inorganic Chemistry*, 6th ed.; Wiley: New York, 1999; pp 468−470.

(8) Kaim, W. *Coord. Chem. Rev.* **2001**, *219−221*, 463.

(9) (a) Doslik, N.; Sixt, T.; Kaim, W. *Angew. Chem.* **1998**, *110*, 2521; *Angew. Chem., Int. Ed.* **1998**, *37*, 2403. (b) Kaim, W.; Doslik, N.; Frantz, S.; Sixt, T.; Wanner, M.; Baumann, F.; Denninger, G.; Kümmerer, H.-J.; Duboc-Toia, C.; Fiedler, J.; Zalis, S. *J. Mol. Struct.* **2003**, *656*, 183.

(10) (a) Kasack, V.; Kaim, W.; Binder, H.; Jordanov, J.; Roth, E. *Inorg. Chem.* **1995**, *34*, 1924. (b) Knödler, A.; Fiedler, J.; Kaim, W. *Polyhedron* **2004**, *23*, 701.

(11) Maji, S.; Sarkar, B.; Patra, S.; Fiedler, J.; Mobin, S. M.; Puranik, V. G.; Kaim, W.; Lahiri, G. K. *Inorg. Chem.* **2006**, *45*, 1316.

(12) Sarkar, B.; Patra, S.; Fiedler, J.; Sunoj, R.; Janardanan, D.; Mobin, S. M.; Niemeyer, M.; Lahiri, G. K.; Kaim, W. *Angew. Chem.* **2005**, *117*, 5800; *Angew. Chem., Int. Ed.* **2005**, *44*, 5655.

Scheme 6

$$L_nM^k(\mu\text{-BL})M^kL_n \; \xrightarrow[\text{MLCT}]{h\nu} \; {}^*[L_nM^{k+1}(\mu\text{-BL}^{\bullet-})M^kL_n]$$

BL: bridging ligand

taken as evidence for a singly reduced, i.e., anion radical bridging ligand, abpy•⁻ in each case, which implies an average oxidation state of 2.5 for the two equivalent metal centers. While valence-localized diruthenium(III,II) or valence-delocalized diruthenium(2.5,2.5) complexes bridged by diamagnetic molecules have been studied in great number,[13] the bridging by an anion radical had not been considered before for ground state situations; however, it was implied for metal-to-ligand charge transfer (MLCT) excited states of acceptor-bridged symmetrically dinuclear complexes (Scheme 6).[14] Very recently, Fabre, Bonvoisin, Launay et al. have proposed a similar situation for a diruthenium complex containing a 1,4-dicyanamidobenzene bridge.[15]

In the following we report studies (electrochemistry, magnetic resonance, spectroscopy, DFT calculations) of the mononuclear reference compound $(abpy)Ru(acac)_2$ (**1**) and give a full description of the *rac* and *meso* isomers (**2**, **3**) of $(acac)_2Ru(\mu\text{-abpy})Ru(acac)_2$, including calculations of geometries, charges, and electronic transitions for the lowest singlet and triplet states. An additional system, $(acac)_2Ru(\mu\text{-abcp})Ru(acac)_2$ (**4**), with the better[9,16] π acceptor 2,2′-azobis(5-chloropyrimidine) = abcp, is presented for which radical complexes of copper(I) and rhenium(I)[17] were structurally characterized by experiment and theory.[9,16] This and the abpy-bridged complexes **2** and **3** have also been studied with respect to their stepwise electrochemical oxidation and reduction within the series $[(acac)_2Ru(\mu\text{-BL})Ru(acac)_2]^n$, $n = -2, -1, 0, +1, +2$, by cyclic voltammetry, EPR, and UV−vis−NIR spectroelectrochemistry. The latter studies are useful to provide frontier MO information and to specify differences based on bridging ligand variation (abpy/abcp) or on configurational isomerism (*rac/meso*). The purpose of these efforts is to confirm the hypothesis of radical ion bridged mixed valent species and to understand the particular electronic structures which are related to the postulated mixed-valent excited-state configurations (Scheme 6).[14] In a wider connection, metal complexes of 1,2-diaryldiazenes such as abpy[8,17,18] have found interest as potentially DNA intercalating chemotherapeutic agents[19] and as photoresponsive species.[20]

Experimental Section

General. The precursor complex $Ru(acac)_2(CH_3CN)_2$[21a] and the ligands 2,2′-azobispyridine (abpy)[8] and 2,2′-azobis-(5-

(13) (a) Kaim, W.; Lahiri, G. K. *Angew. Chem.* **2007**, *119*, 1808; *Angew. Chem., Int. Ed.* **2007**, *46*, 1778. (b) Creutz, C. *Prog. Inorg. Chem.* **1983**, *30*, 1. (c) Richardson, D. E.; Taube, H. *Coord. Chem. Rev.* **1984**, *60*, 107. (d) Crutchley, R. J. *Adv. Inorg. Chem.* **1994**, *41*, 273. (e) Demadis, K. D.; Hartshorn, D. C.; Meyer, T. J. *Chem. Rev.* **2001**, *101*, 2655.

(14) (a) Dattelbaum, D. M.; Hartshorn, C. M.; Meyer, T. J. *J. Am. Chem. Soc.* **2002**, *124*, 4938. (b) Kaim, W.; Kohlmann, S. *Inorg. Chem.* **1987**, *26*, 68. (c) Ernst, S. D.; Kaim, W. *Inorg. Chem.* **1989**, *28*, 1520. (d) For excited state mixed valency of mononuclear complexes with two equivalent charge transfer active ligands, see: Plummer, E. A.; Zink, J. I. *Inorg. Chem.* **2006**, *45*, 6556.

(15) (a) Fabre, M.; Jaud, J.; Hliwa, M.; Launay, J.-P.; Bonvoisin, J. *Inorg. Chem.* **2006**, *45*, 9332. (b) Fabre, M.; Bonvoisin, J. *J. Am. Chem. Soc.* **2007**, *129*, 1434.

(16) Frantz, S.; Hartmann, H.; Doslik, N.; Wanner, M.; Kaim, W.; Kümmerer, H.-J.; Denninger, G.; Barra, A.-L.; Duboc-Toia, C.; Fiedler, J.; Ciofini, I.; Urban, C.; Kaupp, M. *J. Am. Chem. Soc.* **2002**, *124*, 10563.

(17) (a) Hartmann, H.; Scheiring, T.; Fiedler, J.; Kaim, W. *J. Organomet. Chem.* **2000**, *604*, 267. (b) Frantz, S.; Fiedler, J.; Hartenbach, I.; Schleid, Th.; Kaim, W. *J. Organomet. Chem.* **2004**, *689*, 3031.

chloropyrimidine)[9] were prepared according to reported procedures. The synthesis and separation of complexes **2** and **3** have been reported elsewhere.[12] Other chemicals and solvents were reagent grade and used as received. For spectroscopic and electrochemical studies HPLC grade solvents were used.

Instrumentation. UV−vis−NIR spectroelectrochemical studies were performed in CH$_3$CN/0.1 M Bu$_4$NPF$_6$ at 298 K using an optically transparent thin layer electrode (OTTLE) cell[21b] in connection with a J&M TIDAS spectrophotometer. FT-IR spectra were taken on a Nicolet spectrophotometer with samples prepared as KBr pellets. ^{1}H NMR spectra were obtained with a 300 MHz Varian FT spectrometer. The EPR measurements were made in a two-electrode capillary tube[18d] with an X-band Bruker system ESP300 spectrometer. Susceptibility was measured with a Faraday balance (CAHN Instruments, serial no. 76240). Cyclic voltammetric, differential pulse voltammetric, and coulometric measurements were carried out using a PAR model 273A electrochemistry system. Platinum wire working and auxiliary electrodes and an aqueous saturated calomel reference electrode (SCE) were used in a three-electrode configuration. The supporting electrolyte was 0.1 M NEt$_4$ClO$_4$, and the solute concentration was ∼10^{-3} M. **Caution:** Perchlorates are potentially explosive and need to be treated with special precaution. The half-wave potential $E°_{298}$ was set equal to $0.5(E_{pa} + E_{pc})$, where E_{pa} and E_{pc} are the anodic and cathodic cyclic voltammetric peak potentials, respectively. A platinum wire-gauze working electrode was used in the coulometric experiments. The elemental analysis was carried out with a Perkin-Elmer 240C elemental analyzer. Electrospray mass spectra were recorded on a Micromass Q-ToF mass spectrometer.

Synthesis of {Ru(acac)$_2$(abpy)} (1). The precursor complex [Ru(acac)$_2$(CH$_3$CN)$_2$] (100 mg, 0.26 mmol) and the ligand abpy (22 mg, 0.12 mmol) were combined in 20 mL of ethanol, and the solution was heated at reflux for 4 h under a dinitrogen atmosphere. The color of the solution gradually changed from orange to dark brown. The solvent was removed, and the residue was subjected to chromatography on a silica gel column. After the initial elution of a red fraction corresponding to [Ru(acac)$_3$] with CH$_2$Cl$_2$/CH$_3$CN (10:1), a second green fraction was eluted with CH$_2$Cl$_2$/CH$_3$CN (5:1) which corresponded to the diastereomeric mixtures of **2** and **3**. Finally, a third purple fraction corresponding to monomeric complex **1** was eluted with CH$_2$-Cl$_2$/CH$_3$CN (3:1). The solid complex **1** was obtained via evaporation of solvent under reduced pressure, yield of 25 mg (20%). Anal. Calcd for C$_{20}$H$_{22}$N$_4$O$_4$Ru: C, 49.68; H, 4.59; N, 11.59. Found: C, 49.71; H, 4.62; N, 11.57. ESI MS (CH$_2$Cl$_2$):

(18) (a) Kohlmann, S.; Ernst, S.; Kaim, W. *Angew. Chem.* **1985**, *97*, 698; *Angew. Chem., Int. Ed. Engl.* **1985**, *24*, 684. (b) Ernst, S. D.; W. Kaim, W. *Inorg. Chem.* **1989**, *28*, 1520. (c) Heilmann, M.; Frantz, S.; Kaim, W.; Fiedler, J.; Duboc, C. *Inorg. Chim. Acta* **2006**, *359*, 821. (d) Kaim, W.; Ernst, S.; Kasack, V. *J. Am. Chem. Soc.* **1990**, *112*, 173. (e) Kaim, W.; Kohlmann, S.; Jordanov, J.; Fenske, D. *Z. Anorg. Allg. Chem.* **1991**, *598/599*, 217. (f) Krejcik, M.; Zalis, S.; Klima, J.; Sykora, D.; Matheis, W.; Klein, A.; Kaim, W. *Inorg. Chem.* **1993**, *32*, 3362. (g) Fees, J.; Hausen, H.-D.; Kaim, W. *Z. Naturforsch.* **1995**, *50b*, 15.
(19) Corral, E.; Hotze, A. C. G.; Tooke, D. M.; Spek, A. L.; Reedijk, J. *Inorg. Chim. Acta* **2006**, *359*, 830.
(20) (a) Esdaile, L. J.; Jensen, P.; McMurtrie, J. C.; Arnold, D. P. *Angew. Chem.* **2007**, *119*, 2136; *Angew. Chem., Int. Ed.* **2007**, *46*, 2090. (b) Mustroph, H.; Stollenwerk, M.; Bressau, V. *Angew. Chem.* **2006**, *118*, 2068; *Angew. Chem., Int. Ed.* **2006**, *45*, 2016. (c) See also: Kume, S.; Murata, M.; Ozeki, T.; Nishihara, H. *J. Am. Chem. Soc.* **2005**, *127*, 490.
(21) (a) Kobayashi, T.; Nishina, Y.; Shimizu, K. G.; Sato, G. P. *Chem. Lett.* **1988**, 1137. (b) Krejcik, M.; Danek, M.; Hartl, F. *J. Electroanal. Chem.* **1991**, *317*, 179.
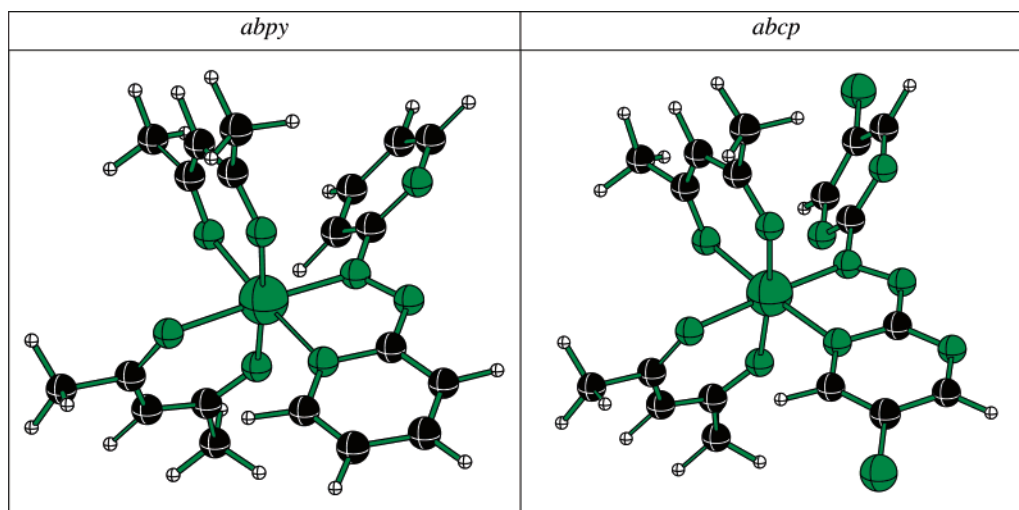
Table 1. Electrochemical and Spectroscopic Data of Complexes

	1	2(*meso*)	3(*rac*)	4
		Cyclic Voltammetry[a]		
$E_{1/2}$ (red 2)	−1.68	−1.67	−1.67	−1.39
$E_{1/2}$ (red 1)	−1.17	−1.03	−1.03	−0.76
$E_{1/2}$ (ox 1)	0.46	0.05	0.05	0.22
$E_{1/2}$ (ox 2)	n.o.	0.89	0.89	1.02
K_c (0)[b]	n.a.	10$^{18.3}$	10$^{18.3}$	10$^{16.6}$
		EPR[c] Anions		
g_1	1.999	1.991	1.991	2.035
g_2	1.999	1.991	1.991	1.990
g_3	1.999	1.991	1.991	1.953
g_1-g_3	<0.05	<0.05	<0.05	0.082
g_{av}[d]	1.999	1.991	1.991	1.993
		EPR[c] Cations		
g_1	2.190	2.347	2.250	2.321
g_2	2.190	2.151	2.140	2.182
g_3	1.914	1.810	1.984	1.843
g_1-g_3	0.276	0.537	0.266	0.478
g_{av}[d]	2.102	2.114	2.128	2.125
		UV−vis−NIR[e]		
$\lambda_{max}(\epsilon)$ [2−]	570 (20 300)	619 (11 700)	620 (11 900)	625sh
	464 (49 600)	501sh	510sh	445 (60 900)
	413 (51 900)		422 (38 400)	
	345 (58 300)	323sh	327sh	
	273 (110 000)	267 (53 100)	272 (83 300)	272 (112 800)
$\lambda_{max}(\epsilon)$ [−]		1780 (2700)	1830 (3100)	1452 (11 100)
	840 (13 200)	1185 (12 400)	1185 (10 900)	740sh
	630 (10 200)	665 (6900)	665 (7400)	518 (23 300)
	453sh	452sh	450sh	
	389 (77 400)	394 (36 000)	396 (39800)	395 (46 200)
	275 (91 400)	268 (51 500)	274 (79 600)	271 (101 200)
$\lambda_{max}(\epsilon)$ [0]	530 (25 000)	848 (29 000)	835 (29 000)	920 (30 000)
	410sh	430sh	430sh	480 (16 600)
	332 (49 100)	340 (39 500)	339 (43 400)	342 (53 400)
	270 (77 900)	270 (52 800)	272 (67 600)	272 (86 500)
$\lambda_{max}(\epsilon)$ [+]	670sh			
	577 (22 200)	655 (22 900)	662 (25 800)	702 (22 100)
	457sh		615sh	
	330sh	300sh	372sh	396 (26 100)
				305sh
	287 (60 300)	272 (44 600)	274 (53 900)	269 (66 400)
$\lambda_{max}(\epsilon)$ [2+]	n.d.	785 (26 300)	801 (29 200)	847 (39 400)
		398 (23 100)	400 (25 000)	404 (30 100)
		291 (40 000)	288 (47 700)	286 (58 100)

^{a} In CH$_3$CN/0.1 M Bu$_4$NPF$_6$. Potentials in V vs Cp$_2$Fe$^{+/0}$. ^{b} K_c = 10$^{\Delta E/59mV}$. ^{c} In CH$_3$CN/0.1 M Bu$_4$NPF$_6$ at 4 K. ^{d} $g_{av} = \sqrt{[(g_1^2 + g_2^2 + g_3^2)/3]}$. ^{e} In CH$_3$CN/0.1 M Bu$_4NPF_6$. λ in nm, ϵ in M^{-1} cm^{-1}.

m/z = 484.26 [M$^+$] (calcd m/z, 484.07). ^{1}H NMR {(CD$_3$)$_2$SO}, δ (J/Hz): 8.51 (d, J = 6.3 Hz, H6), 8.47 (d, J = 8.2 Hz, H3), 8.19 (d, J = 6.4 Hz, H6′), 7.96 (t, J = 6.7 and 8.1 Hz, H5), 7.84 (t, J = 6.4 and 7.8 Hz, H4), 7.61 (d, J = 8.1 Hz, H3′), 7.51 (m, H4′ and H5′), 5.51 (s, CH(acac)), 5.18 (s, CH(acac)), 2.32 (s, CH$_3$(acac)), 1.73 (s, CH$_3$(acac)), 1.71 (s, CH$_3$(acac)), 1.61 (s, CH$_3$(acac)).

Synthesis of {(μ-abcp)[Ru(acac)$_2$]$_2$} (4). The precursor complex [Ru(acac)$_2$(CH$_3$CN)$_2$] (100 mg, 0.26 mmol) and the ligand abcp (34 mg, 0.13 mmol) were mixed in 20 mL of ethanol, and the solution was heated to reflux for 7 h under a dinitrogen atmosphere. The color of the solution changed from orange to dark brown. The solvent was removed, and the residue was subjected to chromatography on a silica gel column. Initially a red compound corresponding to [Ru(acac)$_3$] was eluted with CH$_2$Cl$_2$/CH$_3$CN (15:1). With CH$_2$Cl$_2$/CH$_3$CN (4:1) a brown band was eluted. After evaporation of the solvent under reduced pressure, **4** could be obtained as an analytically pure solid. ^{1}H NMR spectroscopy revealed a mixture of the *meso* and *rac* diastereomers (2:1), but these could not be separated even after careful chromatographic experiments. Yield: 40 mg (18%).

Figure 1. DFT calculated energy minimum structures of (abpy)Ru(acac)$_2$ (**1**, left) and (abcp)Ru(acac)$_2$ (right).

Anal. Calcd for C$_{28}$H$_{32}$Cl$_2$N$_6$O$_8$Ru$_2$: C, 39.40; H, 3.78; N, 9.84. Found: C, 39.36; H, 3.81; N, 9.82. ESI MS (CH$_2$Cl$_2$): m/z = 854.02 [M$^+$] (calcd m/z, 852.98). ^{1}H NMR (*meso*) {(CD$_3$)$_2$SO}, δ (*J*/Hz): 8.60 (s), 8.59 (s), 8.21 (s), 8.20 (s), 5.60 (s, CH-(acac)), 5.31 (s, CH(acac)), 2.32 (s, CH$_3$(acac)), 2.13 (s, CH$_3$-(acac)), 2.06 (s, CH$_3$(acac)), 1.97 (s, CH$_3$(acac)). ^{1}H NMR (*rac*) {(CD$_3$)$_2$SO}, δ (*J*/Hz): 8.61 (s), 8.596 (s), 8.23 (s), 8.22 (s), 5.55 (s, CH(acac)), 5.21 (s, CH(acac)), 2.30 (s, CH$_3$(acac)), 2.12 (s, CH$_3$(acac)), 1.98 (s, CH$_3$(acac)), 1.94 (s, CH$_3$(acac)).

Computational Details. Full geometry optimizations of the complexes were carried out using the density functional theory method at the B3LYP level.[22] All atoms except ruthenium were assigned a 6-31G* basis set. The SDD basis set with effective core potential was employed for the Ru atoms.[23] Calculations were performed with Gaussian98 and Gaussian03 program packages.[24] Optimized geometries were then used for the Natural Bond Orbital (NBO) analysis with the NBO 3.1 program[25] as implemented in the Gaussian suite. Vertical electronic excitations based on B3LYP optimized geometries were computed using the time-dependent density functional theory (TD-DFT) formalism[26] with the B3LYP functional using the above combination of basis sets. Visual inspection of key orbitals was done with MOLDEN[27] to assign the nature of various electronic transitions. Molecular orbital compositions were analyzed using the AOMIX program.[28]

Results and Discussion

Mononuclear Reference Systems. For reference purposes in relation to the dinuclear complexes **2** and **3** we isolated the mononuclear (abpy)Ru(acac)$_2$ (**1**). This complex exhibits

conventional[18b,d,f] electron transfer behavior: The one-electron oxidation produces a ruthenium(III) species as evident from the typical[29] EPR response for a low-spin 4d^5 system (Table 1) with g_1,g_2 > 2 and g_3 < 2 in frozen solution while the first one-electron reduction leads to a $g \approx 2.00$ signal, signifying an abpy$^{\bullet-}$ radical anion complex[30] of ruthenium(II).[18d] These experimental results are supported by DFT calculations which yield a metal centered HOMO (62% Ru) and an abpy centered LUMO (74% abpy, Table S1). Accordingly, the observed absorptions in the visible (Table 1) are assigned to MLCT transitions (570, 464, 413 nm) and are reproduced by TD-DFT calculations (516, 427, 402 nm; Table S2), the difference being attributed to solvent effects. In comparison[18b,f] to [(abpy)Ru-(bpy)$_2$]$^{2+}$ the redox potentials from cyclic voltammetry illustrate that the replacement of the bpy acceptors by acac$^-$ donors causes shifts to more negative potentials by 0.6−0.8 V for reduction and by 1.1 V for the oxidation. Spectroelectrochemistry in the UV−vis region shows the emergence of absorptions at lower energies on reduction and oxidation, the assignment of which as based on related systems[18f] will be discussed in connection with the dinuclear species.

In the absence of single crystalline material, DFT calculations of (abpy)Ru(acac)$_2$ and of the analogous (abcp)Ru(acac)$_2$ yield twisted conformations as optimized geometries (Figure 1, Table S3) with shorter Ru−N$_{azo}$ than Ru−N$_{py}$ bonds (N$_{py}$ = hetero-cyclic N).[18g,19] The NNCN torsional angles reflecting the twisting between chelating and free heterocycles amount to 46.6° (abpy complex **1**) and 57.3° (abcp analogue) while the shorter Ru−N$_{azo}$ bonds illustrate the stronger d(Ru) → π* back-donation to the stronger π accepting function.[18] At about 1.30 Å the calculated N=N bonds are rather long but still more similar to those ($\leq$1.304 Å) of unreduced ruthenium(II),[18g,19] molybdenum-(0),[18e] copper(I),[18e] or rhenium(I)[17] compounds than that of EPR-certified copper(I) radical anion complexes of abcp (1.345(7) Å)[9] or abpy (1.317(1) Å)[31] or calculated rhenium(I) complexes of abpy or abcp ($\approx$1.36 Å).[16] These results suggest a strong amount of π back-donation from one Ru^{II}(acac)$_2$ complex

(22) (a) Becke, A. D. *Phys. Rev. A* **1988**, *38*, 3098. (b) Lee, C.; Yang, W.; Parr, R. G. *Phys. Rev. B* **1988**, *37*, 785.
(23) (a) Andrae, D.; Häußermann, U.; Dolg, M.; Stoll, H.; Preuß, H. *Theor. Chim. Acta* **1990**, *77*, 123. (b) Fuentealba, P.; Preuss, H.; Stoll, H.; Szentpály, L. v. *Chem. Phys. Lett.* **1982**, *89*, 418.
(24) (a) Frisch, M. J. et al. *Gaussian 98*, revision A.11.4; Gaussian, Inc.: Pittsburgh, PA, 2001 (b) Frisch, M. J. et al. *Gaussian 03*, revision C.02; Gaussian, Inc.: Wallingford, CT, 2004.
(25) (a) Glendening, E. D.; Reed, A. E.; Carpenter, J. E.; Weinhold, F. *NBO*, version 3.1. (b) Reed, A. E.; Curtiss, L. A.; Weinhold, F. *Chem. Rev.* **1988**, *88*, 899.
(26) Casida, M. In *Recent Advances in Density Functional Methods*; Chong, D. P., Ed.; World Scientific Press: Singapore, 1995; Vol. I, p 155.
(27) Schaftenaar, G.; Noordik, J. H. *J. Comput.-Aided Mol. Des.* **2000**, *14*, 123.
(28) (a) Gorelsky, S. I. *AOMIX* program, http://www.sg-chem.net/. (b) Gorelsky, S. I.; Lever, A. P. B. *J. Organomet. Chem.* **2001**, *635*, 187.
(29) Hariram, R.; Santra, B. K.; Lahiri, G. K. *J. Organomet. Chem.* **1997**, *540*, 155.
(30) Kaim, W. *Coord. Chem. Rev.* **1987**, *76*, 187.
(31) Roy, S.; Sarkar, B.; Lissner, F.; Schleid, T.; Lahiri, G. K.; Duboc, C.; Fiedler, J.; Kaim, W. Unpublished results.
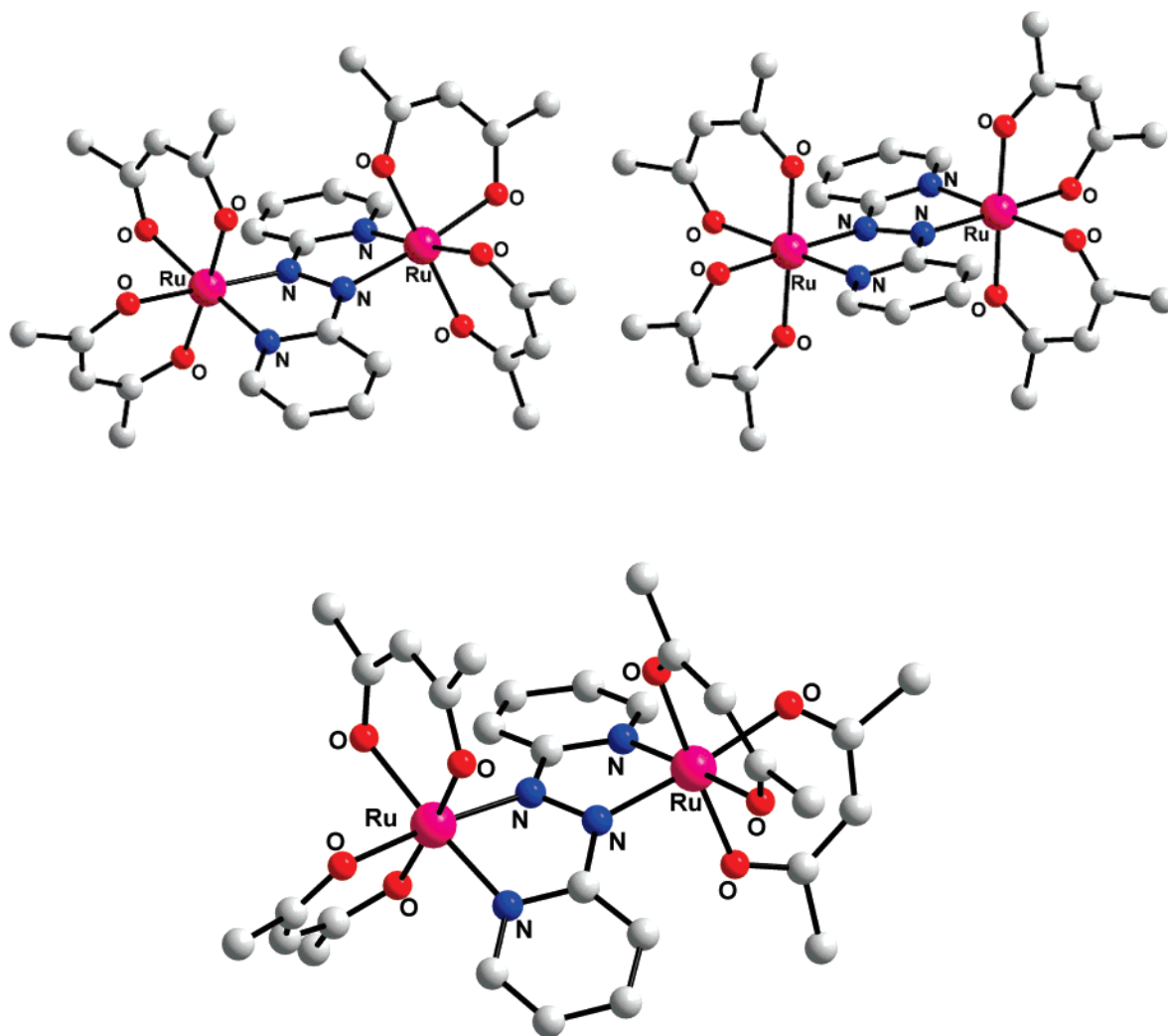
Figure 2. Experimentally determined configurations of complexes **2** (top, two crystallographically independent molecules found, ref 12) and **3** (bottom).
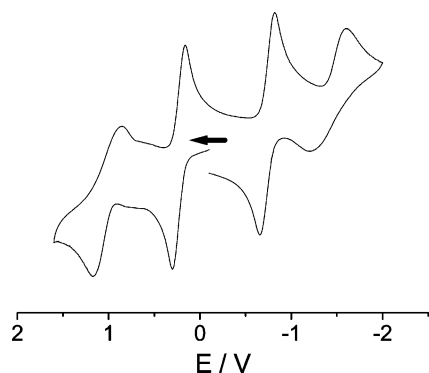

Figure 3. Cyclic voltammogram of **4** in CH₃CN/0.1 M Bu₄NPF₆ at 298 K (100 mV/s scan rate).

fragment into the low lying π^* orbitals of abpy or abcp yet not sufficient for complete reduction.

Dinuclear Compounds: Structures. The two structurally characterized[12] isomers, *meso* (**2**) and *rac* (**3**), of (μ-abpy)[Ru-(acac)₂]₂ (Figure 2) and the isomer mixture **4** of (μ-abcp)[Ru-(acac)₂]₂ were characterized by ¹H NMR and were subjected to cyclic voltammetry (Table 1, Figure 3), EPR and UV−vis−NIR spectroelectrochemistry (Table 1, Figures 4−7) and were calculated using DFT and TD-DFT methodology (Tables 2−8, S4−S10, Figures 8 and 9). Geometry optimizations for both

isomers of (μ-abpy)[Ru(acac)₂]₂ were performed for the lowest singlet and triplet ground states, the values for the singlet forms showing excellent agreement with the experimental parameters for diamagnetic **2** and **3** (Table 2).[12] The calculations for (μ-abcp)[Ru(acac)₂]₂ gave slightly longer NN and shorter C−NN and Ru−N bonds, confirming a more pronounced transfer of negative charge to the bridge. From the excellent structural agreements for **2** and **3** we conclude that the other calculated properties, e.g., orbital energies and orbital compositions as well as transition energies are also reproducing the electronic situation in a proper way.

The experimental and calculated NN distances for the *meso* and *rac* forms (**2**,**3**) of complex (μ-abpy)[Ru(acac)₂]₂ lie in the range corresponding to the anion radical state, i.e., about halfway[33] between the values for unreduced azo N=N bonds[16−19] and those of 2e-reduced NN, i.e., hydrazido(2−) bonds[32] (Scheme 7).

In particular, the structural response of azopyridine bis-chelate ligands such as abpy and abcp on electron addition has been

(32) (a) Marabella, C. P.; Enemark, J. H.; Newton, W. E.; McDonald, J. W. *Inorg. Chem.* **1982**, *21*, 623. (b) Ittel, S. D.; Ibers, J. A. *Inorg. Chem.* **1973**, *12*, 2290. (c) Muñiz, K.; Nieger, M. *Angew. Chem.* **2006**, *118*, 2363; *Angew. Chem., Int. Ed.* **2006**, *45*, 2305.
(33) Shivakumar, M.; Pramanik, K.; Ghosh, P.; Chakravorty, A. *Inorg. Chem.* **1998**, *37*, 5968.
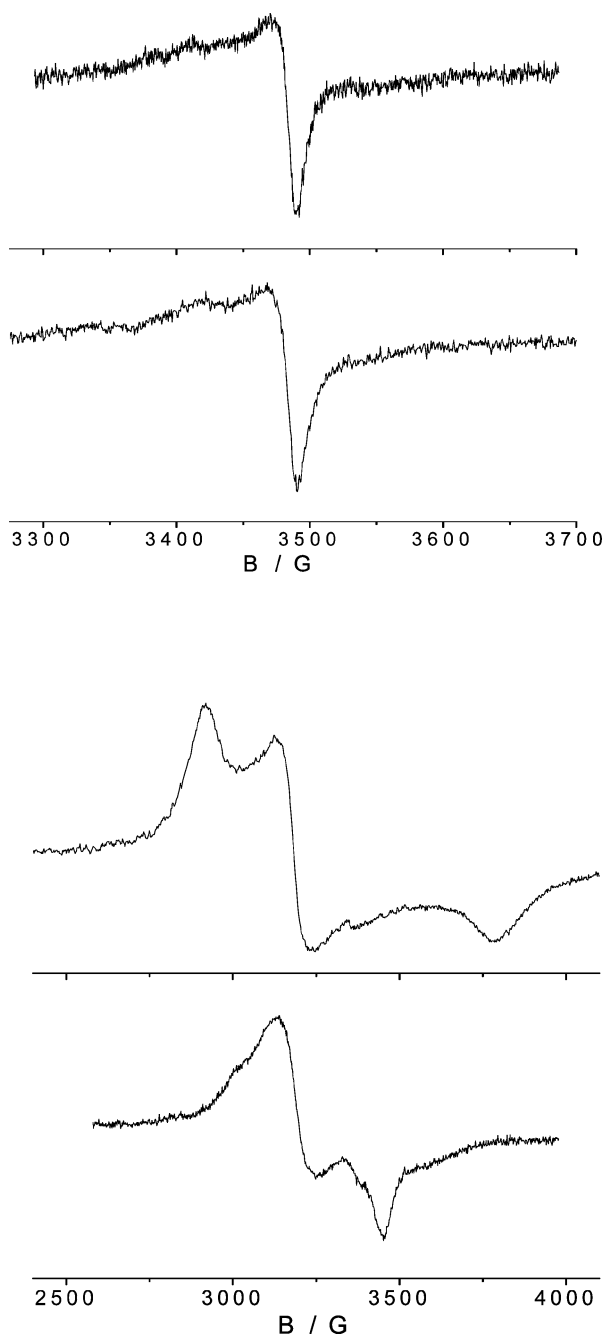
Figure 4. EPR spectra of **2**[•−], **3**[•−], **2**[•+], and **3**[•+] at 4 K in CH$_3$CN/0.1 M Bu$_4$NPF$_6$ (from top to bottom).

well documented for dinuclear bis(phosphino)copper(I) complexes: Whereas {(μ-abpy)[Cu(PPh$_3$)$_2$]$_2$}(BF$_4$)$_2$ has a typical azo ligand structure pattern with d(N=N) = 1.25 Å and d(C−NN) = 1.45 Å,[18e] the one-electron reduced species {(μ-abpy)-[Cu(dppf)]$_2$}(BF$_4$), dppf = 1,1′-bis(diphenylphosphino)ferrocene, has d(N=N) = 1.32 Å and d(C−NN) = 1.38 Å[31] and {(μ-abcp)[Cu(PPh$_3$)$_2$]$_2$}(PF$_6$) has d(N=N) = 1.35 Å and d(C−NN) = 1.36 Å (averaged/rounded values).[9] These bond lengths are not compatible, on the other hand, with an abpy$^{2−}$ formulation which would imply a N−N single bond at >1.40 Å as found for hydrazido(2−) complexes.[11,32] While the increase of d(N=N) and the decrease of d(C−NN) within the ligand are expected for a reduced abpy or abcp molecule (Table 3)[16] or for the related mononucleating 2-phenylazopyridine radical anion (d(N=N) = 1.333(7) Å in a Ru^{II} complex[33]), the decrease

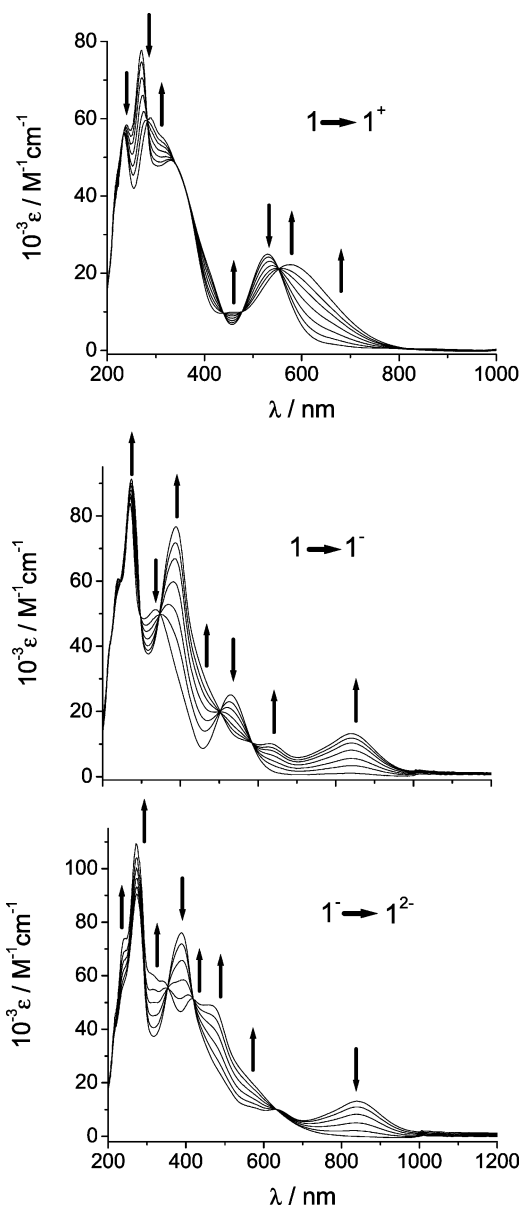**Figure 5.** UV−vis−NIR spectroelectrochemical response of **1** on oxidation (top) and reduction (two steps, bottom) in CH$_3$CN/0.1 M Bu$_4$NPF$_6$.

of the Cu−N distances from about 2.10 Å for {(μ-abpy)[Cu-(PPh$_3$)$_2$]$_2$}(BF$_4$)$_2$ to ca. 2.05 Å for {(μ-abpy)[Cu(dppf)]$_2$}(BF$_4$) also reflects the enhanced charge-based attraction between cationic copper(I) and the now monoanionic ligand bridge. X-band (9.5 GHz) and high-field EPR at 285 GHz have clearly confirmed the abpy$^{•−}$/(Cu^{I})$_2$ oxidation state situation for the one-electron reduced paramagnetic complexes.[9,31]

Using the bis(diphosphinocopper(I)) complexes[9,18e,31] as an unambiguous standard, the amount of (ruthenium)-to-(azo ligand) electron transfer which causes the structural changes as observed experimentally (**2,3**) and as calculated for **2**−**4** (Table 2) corresponds to about one electron. Tables 3 and 4 contain calculated structures, charges, and orbital occupancies which confirm this notion.

The DFT calculated values differ only slightly from the experimental data which provides confidence in the computational results. Moreover, the bond distances vary only marginally between the *meso*(**2**) and *rac*(**3**) configured isomers, indicating that the bond length structural manifestation of the metal−
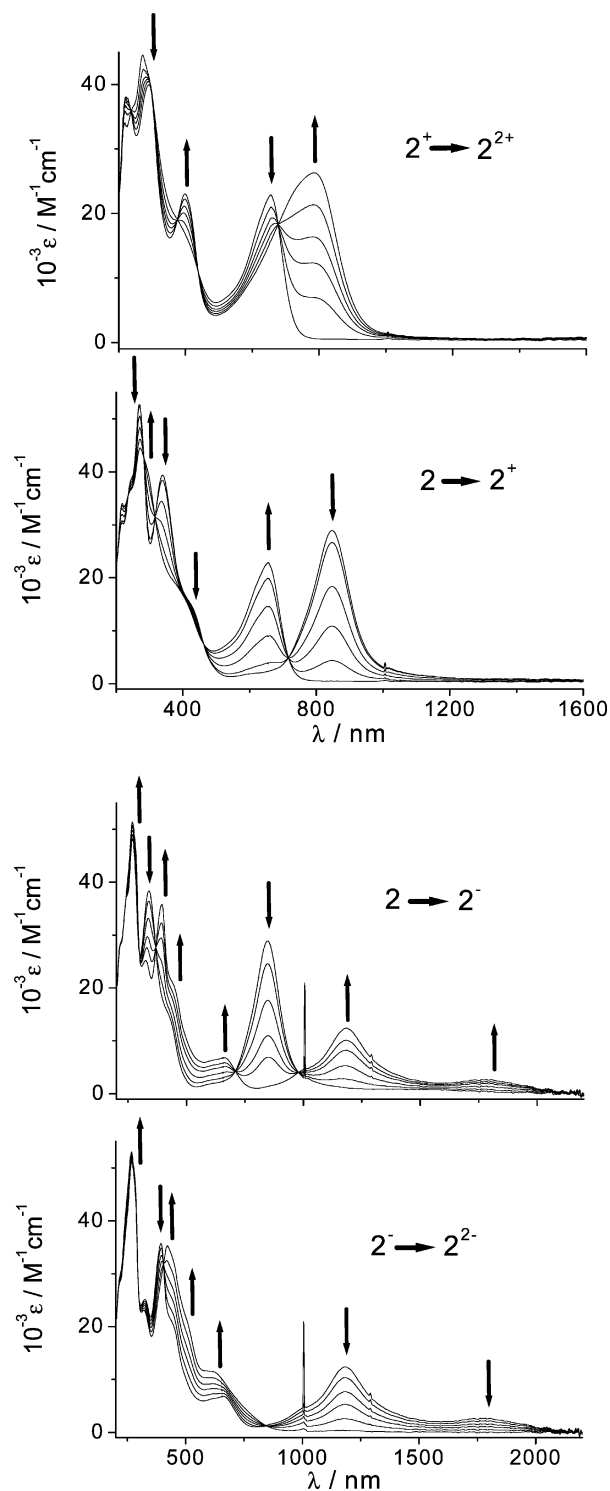
Figure 6. UV−vis−NIR spectroelectrochemical response of **2** on stepwise oxidation (top) and reduction (bottom) in CH₃CN/0.1 M Bu₄NPF₆.

ligand−metal interaction is not too sensitive regarding this kind of isomerism.

However, an interesting aspect is the experimental variability of the *twisting* of the central ligand which is different between the *meso* and *rac* isomers but also within the crystal of **2**.[12] This result and the lesser agreement with the calculated twisting (Table 2) suggest a fairly shallow energy surface for this structural mode, depending largely on intermolecular influences (packing forces). The equilibration of N=N double bonds and C−NN single bonds on reduction to a ligand describable as
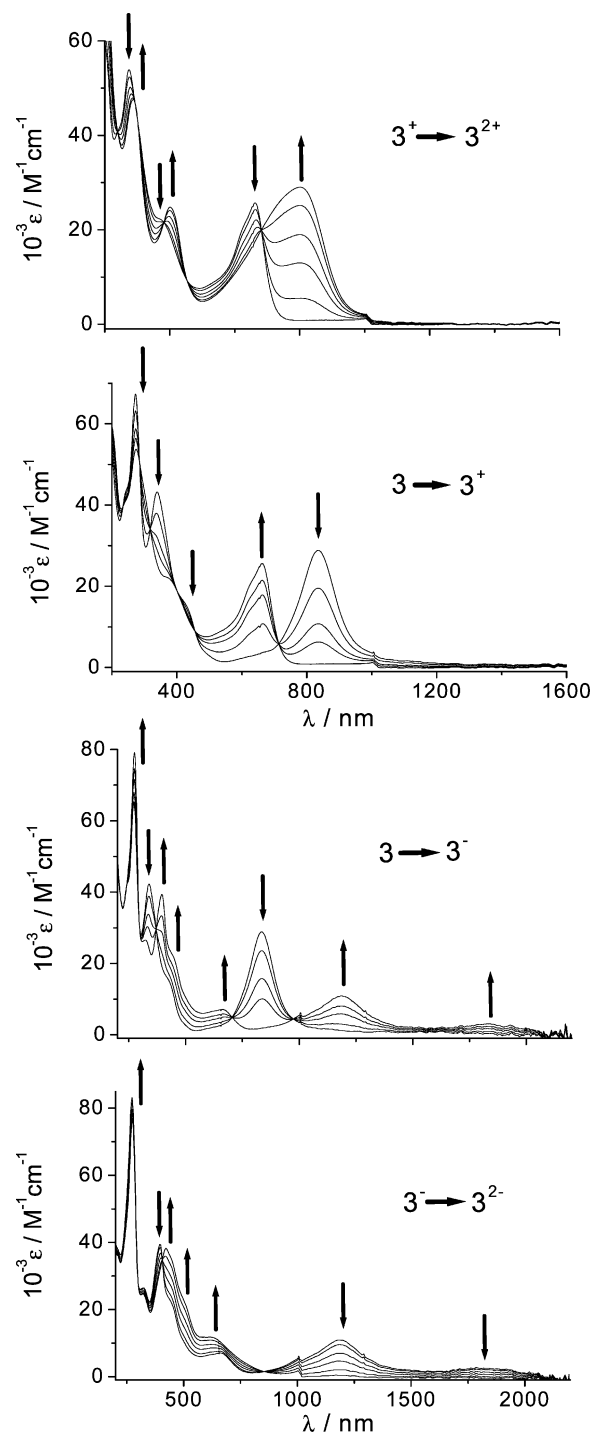
Figure 7. UV−vis−NIR spectroelectrochemical response of **3** on stepwise oxidation (top) and reduction (bottom) in CH₃CN/0.1 M Bu₄NPF₆.

anion radical abpy•⁻ helps to lower barriers for torsional movements and thus allows greater susceptibility for twisting.

The validity of the calculations was further established by TD-DFT computed transition energies for complexes **2**−**4** (Tables 6−8). The values obtained for intense transitions at about 800 nm agree well with the observed band maxima at ca. 900 nm (Table 1, cf. Figures 6, 7), suggesting the suitability of the calculations for these compounds. According to TD-DFT (Tables 6−8) the intense transitions are from filled Ru(acac)₂-based orbitals to azo π*/Ru-centered unoccupied MOs, indicating a mixed IVCT/MLCT type transition (IVCT = intervalence charge transfer); typical delocalized frontier MOs are depicted

Table 2. Essential Structure Parameters of Complexes from Experiment[a] and DFT Calculations[b]

	1	2[d]	3	4[e]
		Bond Lengths (Å)		
N—N	1.300	1.339 (1.363)	1.344 (1.372)	1.352
C—N(≡N)	1.375/1.438	1.391 (1.398)	1.390 (1.390)	1.381
Ru—N$_{azo}$	1.963	2.029 (1.973)	2.014 (1.959)	2.005
Ru—N$_{py}$[c]	2.041	2.021 (2.008)	2.027 (2.008)	2.015
		Torsional Angles (deg)		
C—N—N—C	1.6	0.0 (15.5/0.0)[d]	18.3 (26.1)	16.9

[a] Averaged values in parentheses, from ref 12. [b] For singlet ground states obtained at the B3LYP/SDD/6-31G* level of calculations. [c] py: 2-pyridine (abpy) or 2-(5-chloropyrimidine) (abcp). [d] Two crystallographically independent molecules in the crystal (ref 12). [e] *meso* configuration.

Table 3. Selected Structure Parameters and NBO Results for the Free and Coordinated abpy Ligand[a]

parameter	abpy	abpy•⁻	abpy in complex 3
		Bond Lengths (Å)	
N2—N3	1.26	1.33	1.34 (1.37)[b]
N3—C16	1.43	1.37	1.39 (1.39)
N4—C16	1.34	1.37	1.36 (1.36)
		Dihedral Angle (deg)	
C15—N2—N3—C16	1.5	0.1	18.3 (26.1)

NBO analysis[c]	abpy	abpy•⁻	abpy in complex 3
		Bond Order	
N2—N3	1.78	1.35	1.30
		Occupancy	
π(N2—N3)	1.90	0.97	1.88
π*(N2—N3)	0.16	0.70	0.73
		Charges	
NPA (N2,N3)	−0.18	−0.29	−0.19
Mulliken (N2,N3)	−0.27	−0.39	−0.36

[a] Structure parameters are from B3LYP/6-31G* optimized geometries. [b] Values in parentheses from experimental X-ray diffraction analysis. [c] NBO analysis was performed at the B3LYP/6-31G* level using the NBO 3.1 program as implemented in Gaussian 03.

Table 4. Electron Occupancy of N=N π Orbitals Using NBO Analysis at the B3LYP/SDD/6-31G* Level

compound	π$_{N=N}$	π*$_{N=N}$
1	1.89	0.50
2 (singlet)	1.88	0.73
3 (singlet)	1.87	0.73
3 (triplet)	0.92	0.70
abpy	1.90	0.16
abpy•⁻	a	b

[a] LP1(N1,N2) = 0.97. [b] LP2(N1,N2) = 0.70.

in Figure 8. Reduction and oxidation described below shed further light on the composition of HOMO and LUMO.

The net transfer of one electron equivalent from the metal(s) to the bridging ligand creates a mixed-valent situation with a formally radical anionic spacer in the electronic ground state. In principle, the mixed valency can result in an unsymmetrical situation Ru^{III}(L•⁻)Ru^{II} with different valences or in a symmetrical alternative Ru$^{2.5}$(L•⁻)Ru$^{2.5}$ with averaged net metal valences. Such electronic arrangements have been referred to before for metal-to-ligand charge transfer (MLCT) *excited states* (Schemes 6 and 8) of symmetrically dinuclear complexes bridged by π acceptor ligands;[14a−c] excited-state mixed valency has recently received attention for mononuclear ruthenium containing systems which involve noninnocent ligands.[14d]

Table 5. Kohn−Sham Orbital Energies and Corresponding Orbital Compositions for Isomeric Complexes **2** (*meso*) and **3** (*rac*) Obtained at the B3LYP/6-31G* Level with Optimized Singlet Ground States

orbital	orbital energy		percentage contributions		
	au	cm⁻¹	Ru	abpy	acac
		Compound 2			
173 (LUMO+2)	−0.029	−6500	3.9	71.9	24.2
172 (LUMO+1)	−0.031	−6900	4.8	85.6	9.6
171 (LUMO)	**−0.098**	**−21 600**	**32.1**	**62.1**	**5.9**
170 (HOMO)	**−0.162**	**−35 600**	**72.2**	**4.8**	**23.0**
169 (HOMO−1)	−0.169	−37 100	64.7	5.1	30.2
168 (HOMO−2)	−0.174	−38 200	67.0	9.9	23.0
		Compound 3			
173 (LUMO+2)	−0.031	−6700	3.6	66.2	30.3
172 (LUMO+1)	−0.032	−7100	4.5	84.0	11.5
171 (LUMO)	**−0.099**	**−21 700**	**33.6**	**60.3**	**6.1**
170 (HOMO)	**−0.160**	**−35 100**	**70.9**	**6.2**	**22.9**
169 (HOMO−1)	−0.171	−37 500	65.5	5.2	29.4
168 (HOMO−2)	−0.176	−38 500	68.0	8.8	23.2

Having established the approximate one-electron reduction of the bridging ligand through experimental structure/oxidation state correlations and through DFT calculations the question of spin coupling needs to be addressed. The molecules **2**−**4** are all diamagnetic as evident from susceptibility measurements; they exhibit ¹H NMR features without unusual shifts or line broadening and no EPR signals.

The interaction between a mixed-valent dimetal arrangement, valence-averaged or not, and an anion radical ligand creates the possibility of singlet or triplet configurations. While the experimental evidence suggests the singlet state as the ground state for **2**−**4**, we used the DFT method to confirm this result and to calculate the energy and properties of the triplet configurations (Tables S5, S7−S10). The triplet states are calculated to lie 1535 cm⁻¹ (**2**) or 840 cm⁻¹ (**3**) above the corresponding singlet ground states, and their computed structures, especially the lengthened NN bonds,[12] reflect decreased NN bonding for the triplet following from a depopulated HOMO (Table 4). The preference for a singlet ground state in such situations may not always be so pronounced; strong interaction between two abpy or abcp bridged metal centers must be favored here because these "S-frame" ligands[8] induce a rather short metal−metal distance of less than 5 Å despite the molecular nature of the bridge.[12] Accordingly, when applying the conventional formalism to calculate the comproportionation constant K_c ($RT \cdot \ln K_c = nF \cdot \Delta E$) to the isolated neutral states, one arrives at large values of about 10¹⁷ (Table 1) which are not so common in diruthenium mixed-valence chemistry.[13]

Dinuclear Compounds: Two-Step Oxidation and Reduction. The opportunity of having two fully reversible one-electron oxidation and reduction processes available for spectroelectrochemical studies (UV−vis−NIR, EPR) provides valuable additional information on the electronic situation in complexes **2**−**4** and their neighboring charged states. Before spectroelectrochemical characterization one may note that the potentials are practically identical for the two disastereoisomers **2** and **3** despite different solid-state structures (Figure 2);[12] the potentials are slightly anodically shifted for system **4** with the better π acceptor bridge (Table 1).

For the EPR spectroscopically accessible monoanions and monocations the shift and anisotropy of the *g* factors in a frozen

Table 6. Selected List of Vertical Excitations Computed at the TD-DFT/B3LYP//B3LYP/SDD/6-31G* Level for **2**

excitation energy[a] (10^3 cm^{-1})	oscillator strength	ϵ^c	$\psi_o - \psi_v{}^d$	type of transition
6.950 (1440)[b]	0.0036	250	HOMO → LUMO (0.54)[e]	dπ (Ru$_1$,Ru$_2$), π(acac) → π*(abpy), dπ (Ru$_1$,Ru$_2$)
13.850 (722)	**0.2146**	**15070**	**HOMO−2 → LUMO (0.50)**	**dπ (Ru$_1$,Ru$_2$), π(acac) → π*(abpy), dπ (Ru$_1$,Ru$_2$)**
20.610 (485)	0.0044	310	HOMO−6 → LUMO (0.69)	π(acac) → π*(abpy), dπ (Ru$_1$,Ru$_2$)
22.430 (446)	0.0051	360	HOMO−8 → LUMO (0.67)	π(acac), dπ (Ru$_1$,Ru$_2$) → π*(abpy), dπ (Ru$_1$,Ru$_2$)
23.070 (434)	**0.0203**	**1430**	**HOMO → LUMO+2 (0.63)**	**dπ (Ru$_1$,Ru$_2$), π(acac) → π*(abpy), π*(acac)**

[a] Singlet excitation energies. [b] Values in nm given in parentheses. [c] ϵ in /M^{-1} cm^{-1}. [d] Occupied and virtual orbitals. [e] Transition coefficients.

Table 7. Selected List of Vertical Excitations Computed at the TD-DFT/B3LYP//B3LYP/SDD/6-31G* Level for **3**

excitation energy[a] (10^3 cm^{-1})	oscillator strength	ϵ^c	$\psi_o - \psi_v{}^d$	type of transition
6.980 (1432)[b]	0.0065	460	HOMO → LUMO (0.51)[e]	dπ (Ru$_1$,Ru$_2$), π(acac) → π*(abpy), dπ (Ru$_1$,Ru$_2$)
13.720 (729)	**0.1910**	**13410**	**HOMO−2 → LUMO (0.47)**	**dπ (Ru$_1$,Ru$_2$), π(acac) → p*(abpy), dπ (Ru$_1$,Ru$_2$)**
18.420 (543)	0.0090	630	HOMO−5 → LUMO (0.64)	π(acac), π(abpy), dπ(Ru$_1$,Ru$_2$) → π*(abpy), dπ (Ru$_1$,Ru$_2$)
20.590 (486)	0.0072	510	HOMO−6 → LUMO (0.69)	π (acac), dπ (Ru$_1$,Ru$_2$) → π*(abpy), dπ (Ru$_1$,Ru$_2$)
22.360 (447)	0.0061	430	HOMO−8 → LUMO (0.67)	π (acac), dπ (Ru$_1$,Ru$_2$) → π*(abpy), dπ (Ru$_1$,Ru$_2$)
22.640 (442)	**0.0123**	**860**	**HOMO → LUMO+2 (0.65)**	**dπ (Ru$_1$,Ru$_2$), π(acac) → p*(abpy), π*(acac)**

[a] Singlet excitation energies. [b] Values in nm given in parentheses. [c] ϵ in /M^{-1} cm^{-1}. [d] Occupied and virtual orbitals. [e] Transition coefficients.

Table 8. Selected List of Vertical Excitations Computed at the TD-DFT/B3LYP//B3LYP/SDD/6-31G* Level for **4**

excitation energy[a] (10^3 cm^{-1})	oscillator strength	ϵ^c	$\psi_o - \psi_v{}^d$	type of transition
6.170 (1621)[b]	0.0024	170	HOMO−2 → LUMO (0.46)[e] HOMO−1 → LUMO (0.42)	dπ(Ru$_2$), π(acac), dπ(Ru$_1$) → π*(abcp), dπ(Ru$_1$,Ru$_2$) dπ(Ru$_1$), π(acac), dπ(Ru$_2$), π(abcp) → π*(abcp), dπ(Ru$_1$,Ru$_2$)
12.180 (821)	**0.1757**	**12 340**	**HOMO−2 → LUMO (0.41)**	**dπ(Ru$_2$), π(acac), dπ(Ru$_1$) → π*(abcp), dπ(Ru$_1$,Ru$_2$)**
16.030 (624)	0.0109	770	HOMO−5 → LUMO (0.65)	π(acac), π(abcp), dπ(Ru$_1$) → π*(abcp), dπ(Ru$_1$,Ru$_2$)
17.390 (575)	0.0080	560	HOMO−6 → LUMO (0.64)	π(acac), dπ(Ru$_1$) → π*(abcp), dπ(Ru$_1$,Ru$_2$)
18.790 (532)	0.0067	470	HOMO → LUMO+1 (0.62)	dπ(Ru$_1$), dπ(Ru$_2$), π(acac) → π*(abcp)
20.440 (489)	**0.0090**	**630**	**HOMO−1 → LUMO+2 (0.43) HOMO−1 → LUMO+1 (0.37)**	**dπ(Ru$_1$), π(acac), dπ(Ru$_2$), π(abcp) → π*(abcp) dπ(Ru$_1$), π(acac), dπ(Ru$_2$), π(abcp) → π*(abcp)**
20.760 (482)	0.0062	440	HOMO−1 → LUMO+1 (0.53)	dπ(Ru$_1$), π(acac), dπ(Ru$_2$), π(abcp) → π*(abcp)
21.250 (471)	0.0065	460	HOMO−9 → LUMO (0.46)	π(acac), dπ (Ru$_2$), π (abcp) → π(abcp), dπ(Ru$_1$,Ru$_2$)

[a] Singlet excitation energies. [b] Values in nm given in parentheses. [c] ϵ in /M^{-1} cm^{-1}. [d] Occupied and virtual orbitals. [e] Transition coefficients.

solution proved to be elucidating. Both **2**$^{•-}$ and **3**$^{•-}$ exhibit no such *g* component splitting in the X band (9.5 GHz), and the value of 1.991, very slightly below 2, is typical for ruthenium-(II) complexes of anion radical ligands.[18d] The oxidation state description Ru^{II}(L$^{•-}$)Ru^{II} is thus considered most appropriate. For **4**$^{•-}$ the g factor components are clearly split (Table 1), suggesting some detectable but minor contribution from the alternative mixed-valent formulation Ru$^{2.5}$(L^{2-})Ru$^{2.5}$ (Scheme

9, valence averaging) with participation from the heavy metals with their considerable spin−orbit coupling constant. However, all three systems **2**$^{•-}$−**4**$^{•-}$ are distinguished by intense NIR absorptions which cannot be due to any IVCT transition but to MLCT transitions from the ruthenium(II) donors to the still π accepting anion radical bridge.[11,34] Notably, this feature is absent for the mononuclear compound **1**$^{•-}$ and is hypsochromically shifted for **4**$^{•-}$ with the more pronounced metal participation

LUMO (**2**)　　　　　HOMO (**2**)
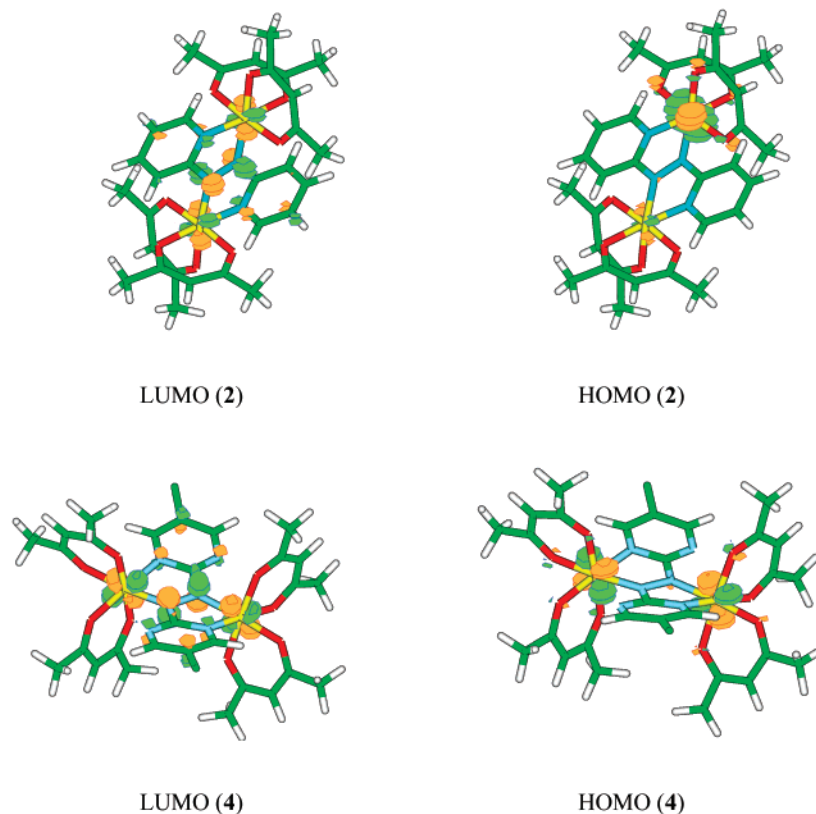

LUMO (**4**)　　　　　HOMO (**4**)

Figure 8. DFT calculated frontier orbitals for compounds **2** and **4**.
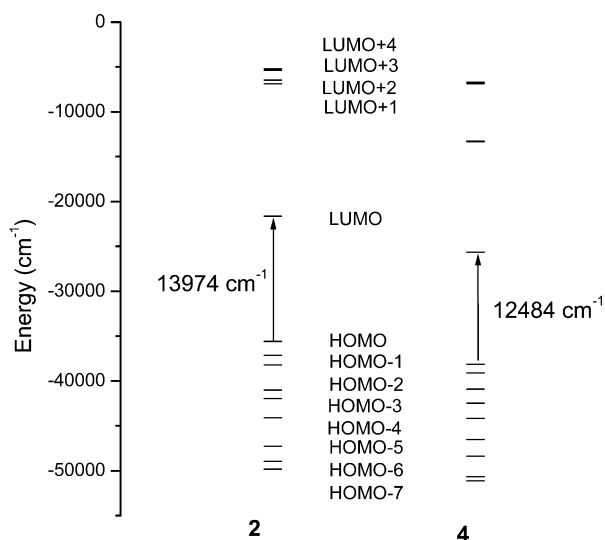

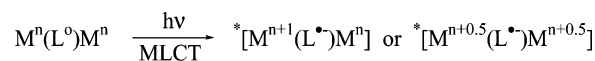***Figure 9.*** DFT calculated MO energy diagrams for compounds **2** and **4**.

as evident from the EPR results. Further reduction can only lead to the $Ru^{II}(L^{2-})Ru^{II}$ state which exhibits intense charge-transfer bands in the visible around 600 and 430 nm, tentatively attributed to MLCT or LLCT with π^*(acac) as the target MO. The more pronounced bridging ligand character of the LUMOs has been calculated by DFT (cf. Table 5, Figure 8).

One-electron oxidation of compounds **2**−**4** produces EPR spectra with pronounced *g* factor shifts and *g* anisotropies. The latter, a very sensitive probe of the electronic structure, shows a clear difference between the two diastereoisomers **2**$^+$ and **3**$^+$,

(34) Ernst, S.; Hänel, P.; Jordanov, J.; Kaim, W.; Kasack, V.; Roth, E. *J. Am. Chem. Soc.* **1989**, *111*, 1733.

Scheme 7

redox state	range of N N bond lengths
$\diagdown N {=\!=} N \diagup$	1.22 - 1.31
$\diagdown N^{\ominus} \overset{\bullet}{{=\!=}} N \diagup$	1.31 – 1.41
$\diagdown N^{\ominus} {-\!-} N^{\ominus} \diagup$	1.41 – 1.50

Scheme 8

$$M^n(L^0)M^n \xrightarrow[\text{MLCT}]{h\nu} {}^*[M^{n+1}(L^{\bullet-})M^n] \text{ or } {}^*[M^{n+0.5}(L^{\bullet-})M^{n+0.5}]$$
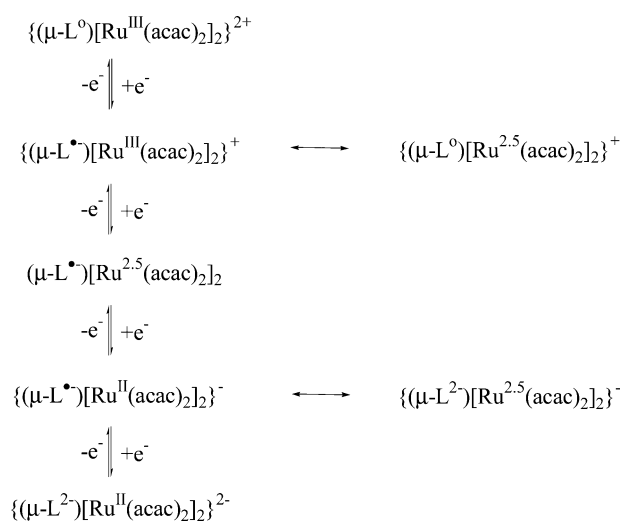
possibly because of different structures as established already for the neutral precursors (Figure 2).[12] Otherwise, the UV/vis/ NIR spectroelectrochemical response of the isomers **2** and **3** is small (Figures 6, 7). Unfortunately, the obviously metal centered spin for the monocations is compatible with two alternative descriptions, starting from the neutral forms: Oxidation of the bridging ligand would produce a classical mixed-valent situation $Ru^{2.5}(L^0)Ru^{2.5}$ with an unreduced nonradical bridge while a metal-based oxidation would create a three-spin[35] arrangement $Ru^{III}(L^{\bullet-})Ru^{III}$ (low-spin ruthenium(III)). Assuming dominant metal−ligand antiferromagnetic interactions the resulting up−down−up arrangement for the spins[35] would leave one net metal-centered spin, just as in the previous alternative. Support

(35) Ye, S.; Sarkar, B.; Lissner, F.; Schleid, Th.; van Slageren, J.; Fiedler, J.; Kaim, W. *Angew. Chem.* **2005**, *117*, 2140; *Angew. Chem., Int. Ed.* **2005**, *44*, 2103.

Scheme 9

$$\{(\mu\text{-}L^o)[Ru^{III}(acac)_2]_2\}^{2+}$$

$$-e^- \,\|\, +e^-$$

$$\{(\mu\text{-}L^{\bullet-})[Ru^{III}(acac)_2]_2\}^+ \quad\longleftrightarrow\quad \{(\mu\text{-}L^o)[Ru^{2.5}(acac)_2]_2\}^+$$

$$-e^- \,\|\, +e^-$$

$$(\mu\text{-}L^{\bullet-})[Ru^{2.5}(acac)_2]_2$$

$$-e^- \,\|\, +e^-$$

$$\{(\mu\text{-}L^{\bullet-})[Ru^{II}(acac)_2]_2\}^- \quad\longleftrightarrow\quad \{(\mu\text{-}L^{2-})[Ru^{2.5}(acac)_2]_2\}^-$$

$$-e^- \,\|\, +e^-$$

$$\{(\mu\text{-}L^{2-})[Ru^{II}(acac)_2]_2\}^{2-}$$

for one of the alternatives from UV–vis–NIR spectroelectrochemistry appears in the form of the absence of detectable NIR absorption which seems to rule out the former, mixed-valent formulation. However, there are dinuclear and trinuclear mixed-valent complexes of $Ru(acac)_2$, bridged by neutral acceptor ligands, which do not exhibit detectable IVCT absorption in the NIR region.[36] We thus cannot assign unambiguously an oxidation state formulation to the monocationic states. On second oxidation we assume the formation of $Ru^{III}(L^0)Ru^{III}$ compounds with intense LMCT absorptions around 800 nm (Figures 6 and 7).

Conclusion

Using two familiar kinds of components in coordination chemistry, viz., ruthenium(II) donors and "polypyridine"-type acceptor ligands, we have been able to show the consequences of excessive donor-to-acceptor transfer of negative charge in corresponding dinuclear complexes $(acac)_2Ru(\mu\text{-}L)Ru(acac)_2$, L = abpy or abcp. The experimentally (structural, spectroscopic)

and computationally established amount of charge shift, corresponding to about one electron, formally creates an unfamiliar situation involving mixed-valency, expounded systematically in 1967,[37] and a bridging ligand existing in anion radical form, as first reviewed in 1987.[30] In this way, a configuration used to describe excited states (Scheme 6) has been obtained as a ground state species, just as mononuclear MLCT excited state-type configurations were established earlier[38] for ground state species. The consequences of this uncommon arrangement are structural flexibility as indicated for both *meso* and *rac* diastereoisomers studied with L = abpy, intense long-wavelength absorptions ascribed to mixed IVCT/MLCT transitions, and relatively small singlet–triplet gaps as calculated by DFT. Reversible oxidation and reduction processes with spectroelectrochemical characterization of the charged species confirm a more pronounced ligand contribution to the LUMO than to the HOMO.

Viewed in connection with previously and currently practiced structure/oxidation state correlations in coordination chemistry involving noninnocently behaving ligands (Schemes 1–5) the present results suggest that, at least for strongly mixing systems such as ruthenium compounds or S-ligand containing complexes,[39] that approach can be seen as a formal exercise which may provide some insight into the electronic structure without warranting a too literal significance of the valence denomination.

Supporting Information Available: Complete ref 24; Tables S1–S10 of DFT and TD-DFT calculation results. This material is available free of charge via the Internet at http://pubs.acs.org.

JA077676F

(36) (a) Patra, S.; Sarkar, B.; Ghumaan, S.; Fiedler, J.; Kaim, W.; Lahiri, G. K. *Dalton Trans.* **2004**, 754. (b) Ghumaan, S.; Sarkar, B.; Patil, M. P.; Fiedler, J.; Sunoj, R. B.; Kaim, W.; Lahiri, G. K. *Polyhedron* **2007**, *26*, 3409. (c) Patra, S.; Sarkar, B.; Ghumaan, S.; Fiedler, J.; Kaim, W.; Lahiri, G. K. *Inorg. Chem.* **2004**, *43*, 6108.

(37) Robin, M. B.; Day, P. *Adv. Inorg. Chem. Radiochem.* **1967**, *10*, 247.
(38) Kaim, W.; Reinhardt, R.; Sieger, M. *Inorg. Chem.* **1994**, *33*, 4453.
(39) Kapre, R. R.; Bothe, E.; Weyhermüller, T.; DeBeer, George, S.; Muresan, N.; Wieghardt, K. *Inorg. Chem.* **2007**, *46*, 7827.